

Ka-band compact multi-materials rectangular waveguide loads

L. Martinez-Cano⁽¹⁾⁻⁽²⁾, A. Chevalier⁽¹⁾, A. Maalouf⁽¹⁾, J. Ville⁽²⁾, J. Bénédicto⁽¹⁾, P. Laurent⁽¹⁾, K. Elis⁽³⁾
and V. Laur⁽¹⁾

⁽¹⁾ *Lab-STICC, Univ. Brest*
6 avenue Victor le Gorgeu 29238 Brest Cedex 3
vincent.laur@univ-brest.fr

⁽²⁾ *IRDL, Univ. Brest*
6 avenue Victor le Gorgeu 29238 Brest Cedex 3

⁽³⁾ *CNES*
18 avenue Edouard Belin 31400 Toulouse

INTRODUCTION

Microwave loads (or terminations) are key devices in many telecommunication systems. In rectangular waveguide technology, these components are constituted of an absorber positioned in a short-circuited waveguide. The shape of the absorber mainly depends on the bandwidth required for a given application. These components are usually associated with a coupler or a circulator. As an example, in satellite and radar systems, isolators (circulator + load) are used to protect components that are sensitive to RF power variations and to impedance mismatch such as amplifiers. Current satellite architectures integrate few microwave terminations. However, in future architectures based on multi-spot technologies, several tens of microwave terminations will have to be integrated due to the parallelization of RF chains. For some of these applications, the main constraint is no longer the return loss level of the load (that can be of the order of 10 dB) but the size of the component that must be minimized.

In the framework of a R&T CNES project, we investigated the feasibility to develop compact rectangular waveguide loads in Ka-band that have to provide a reflection coefficient lower than -15 dB between 35.5 GHz and 36 GHz. Lab-STICC and IRDL developed a few years ago a new technology to manufacture these components. This technology is based on a 3D printing technique of polymer composites that can be used to manufacture rectangular waveguide loads [1]-[2]. This technology was already used to manufacture free-space microwave absorbers [3].

In this paper, we will present new 3D-printed loads dedicated to Ka-band applications. At first, a carbon-filled acrylonitrile butadiene styrene (ABS-ESD) material will be used to design standard wedge loads. These components will be measured and compared to simulations and their temperature stability will be evaluated. Then, a new compact design based on a resonant Salisbury principle will be described. Different components will be manufactured and measured in order to confirm the validity of this new approach.

3D-PRINTING TECHNOLOGY

Several families of 3D-printing technologies are now finding industrial applications in the fields of health, aeronautics and the automotive industry for example. Applications are also being developed in the field of telecommunications for the manufacture of components and structures. Among them, Fused Deposition Modeling (FDM) appears to be one of the most common and cheapest additive technologies. This 3D printing technique consists in manufacturing an object layer-by-layer using an extruder that pushes the material, in the form of a filament, through a nozzle that can move in a plane over a heated bed (Fig. 1). At first, a 3D model of the object to be printed is converted to a gcode command file by using a slicing software. This file contains motor controls (X, Y, Z movements, extruder rotations) and temperatures (nozzles, bed and chamber). The temperature-controlled extrusion head is fed with a thermoplastic material that is heated at a temperature above its fusion one. The material is deposited in layers with typical thickness of 100-200 μm and the part is built from the bottom, layer by layer. The material hardens immediately after extrusion and the bed goes down between each layers. We used a 3NTR A2v3 printer to manufacture our devices.

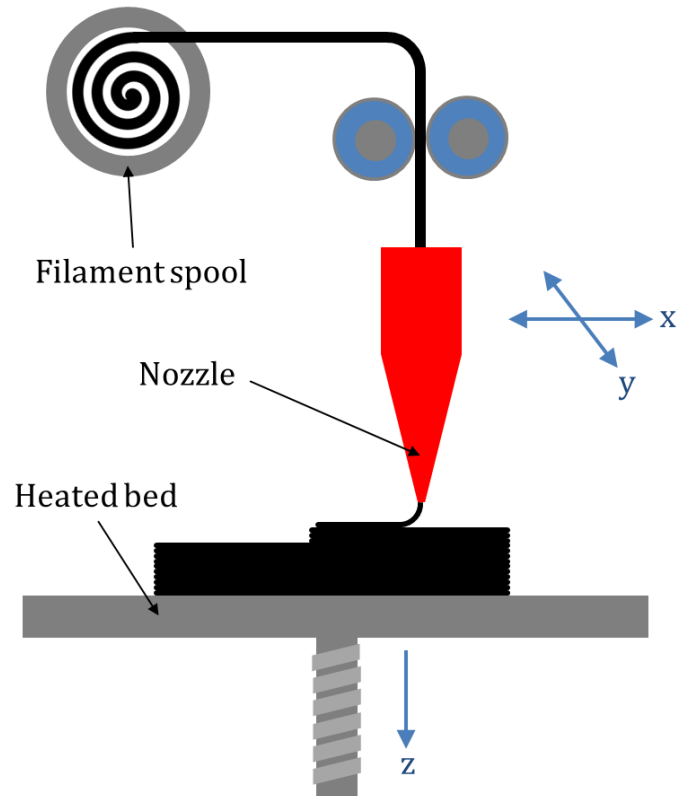


Fig. 1. Fused Deposition Modeling principle

At first, our interest was focused on a carbon-filled Acrylonitrile Butadiene Styrene (ABS) developed to avoid ElectroStatic Discharge (ESD). This material, provided by Nanovia, was printed at a bed temperature of 110°C and a nozzle temperature of 240°C with a thickness layer of 100 μm . This material was characterized at Ka-band using a rectangular waveguide method and its dielectric properties were evaluated to be around $\epsilon_r = 8$ and $\tan\delta = 0.3$.

DESIGN, MANUFACTURING AND EVALUATION OF 3D-PRINTED WEDGE LOADS

Ansys HFSS software was used to design wedge loads compatible with a standard WR-28 rectangular waveguide. FDM technology will allow us to not only manufacture the wedge but also its flange (UBR 320 / IEC 60154) so that the component can be directly connected to a metallic waveguide. In practice, the back face of the component will be metallized using a silver lacquer in order to ensure a total reflection and to avoid a potential leakage of electromagnetic wave. In simulation, this silver lacquer layer was simulated by using a Finite Conductivity Boundary with a conductivity $\sigma = 5.10^6$ S/m.

The simulation model is presented in Fig. 2. In our case, the component is defined by 3 main dimensions: the height of the top of the wedge h_{tw} , the length of the wedge l_w and the thickness of the flange e_f . The first parameter h_{tw} is imposed by the manufacturing process. Indeed, as the component is manufactured layer-by-layer from the flange to the top of the wedge, h_{tw} cannot be thinner than the nozzle diameter. Here, h_{tw} was fixed to a value of 0.6 mm. The thickness of the flange e_f was also fixed to 1 mm. Fig. 2 presents the simulated reflection coefficient of the load for different wedge lengths l_w . For $l_w = 3$ mm, the specifications ($S_{11} < -15$ dB between 35.5 and 36 GHz) are not achieved. For longer wedges, the frequency of maximum absorption is moving toward a lower frequency and it was observed that a wideband behavior is obtained for $l_w = 7$ mm. As our objective is to get a compact component, $l_w = 4$ mm was selected because it allows achieving the specifications with the lowest total length (5 mm).

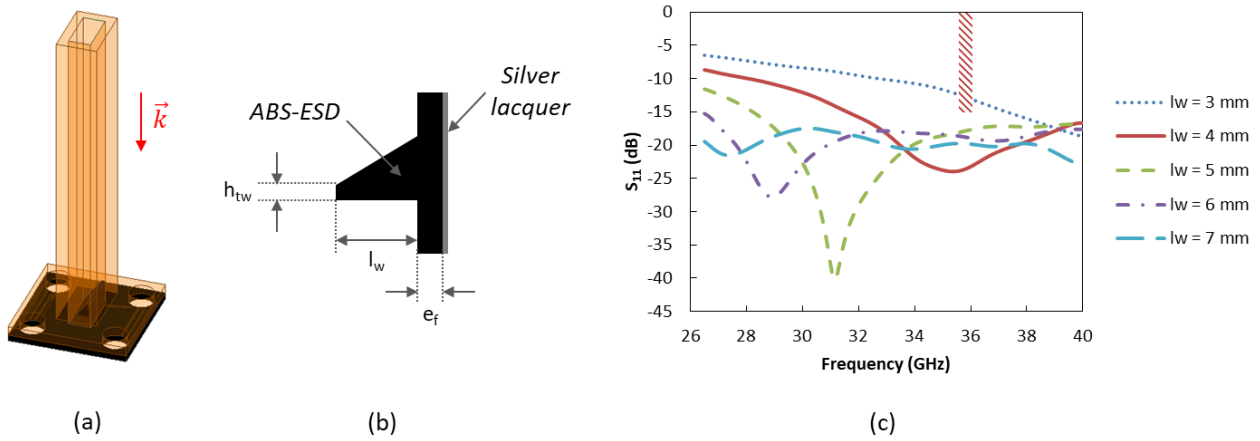


Fig. 2. (a) Simulation model with \vec{k} the propagation direction, (b) side view of the wedge load and (c) amplitude of the reflection coefficient S_{11} in Ka-band for different wedge lengths l_w ($h_{tw} = 0.6$ mm, $e_f = 1$ mm). The shaded zone corresponds to the specifications.

This component was 3D-printed using a A4v3 printer with the printing conditions detailed in the previous section. After manufacturing, a silver lacquer was applied to the back face of the component. In order to remove the solvents, the component was then dried at 60°C during one hour. One should note that the final component is very light with a mass of only 0.42 g.

A Rohde & Schwarz ZVA 67 vector network analyzer was used to measure the reflection coefficient of the load. A Thru-Reflect-Line calibration was first performed in order to put the reference plane of measurement at the output of the coaxial-to-rectangular waveguide transition. Fig. 3 presents a comparison between simulated and measured reflection coefficients in Ka-band. A 700 MHz shift toward low frequencies was observed. The real dimensions of the load were measured and considered in simulations. Considering a wedge length of 4.2 mm and a flange thickness of 0.92 mm, a better agreement is achieved between the retro-simulated and measured frequencies of maximum absorption. However, a slight difference is already observed between the levels of minimum reflection coefficient. Nevertheless, specifications are experimentally achieved with S_{11} lower than -22.6 dB between 35.5 GHz and 36 GHz for a total measured length of 5.12 mm.

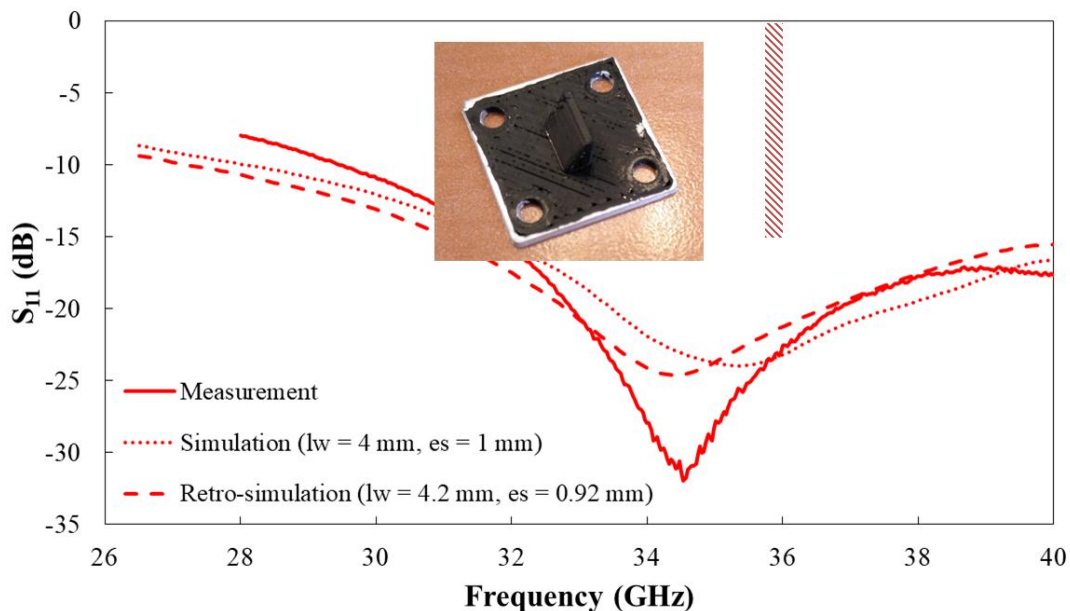


Fig. 3. Comparison between simulated, measured and retro-simulated reflection coefficient of a 3D-printed wedge load in Ka-band.

This component was then measured in a climatic chamber in order to evaluate its temperature stability. Fig. 4 presents the reflection coefficient of this component for temperatures ranging from -20°C and 60°C . These measurements were noisier than the previous ones due to calibration difficulties in the climatic chamber. However, they demonstrate a high temperature stability of the reflection coefficient in this temperature range. A slight increase of S_{11} is observed between 37 GHz and 38.5 GHz at high temperature but the specifications remain achieved from -20°C to 60°C .

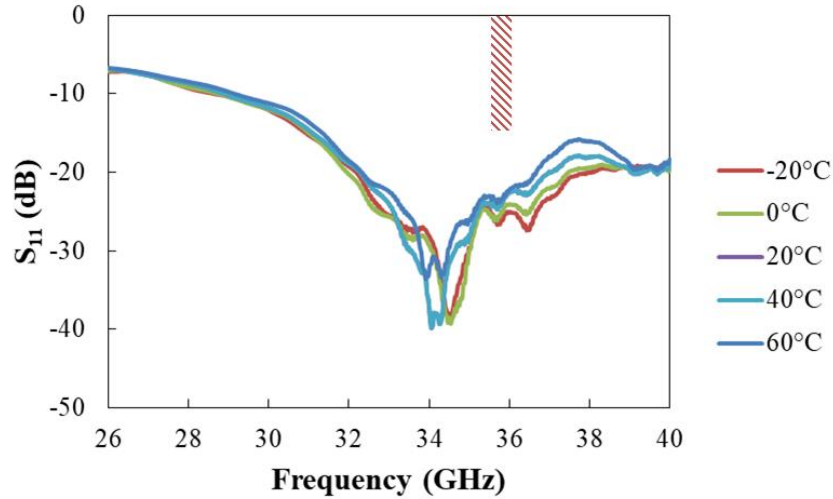


Fig. 4. Measured reflection coefficient of a 3D-printed wedge load in Ka-band for temperatures between -20°C and 60°C .

COMPACT TOPOLOGY OF RESONANT 3D-PRINTED LOADS

The concept of this new topology is based on the Salisbury absorber in free-space. This absorber screen is constituted of a dielectric spacer with thickness e_s and a resistive film with conductivity σ and thickness τ (Fig. 5). The back face of the structure is metallized in order to ensure a total reflection of EM waves. When the thickness of the spacer is equal to the quarter of the wavelength, a constructive interference occurs at the top of the spacer layer. If the thickness of the resistive layer is adjusted to present an impedance equal to the one of air ($Z_s = 377 \Omega$), a strong absorption is achieved.

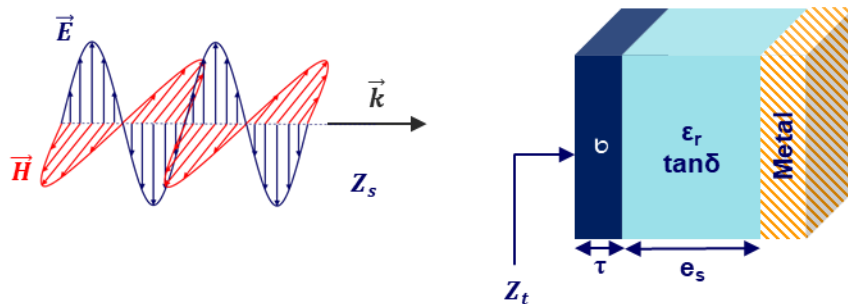


Fig. 5. Illustration of a standard Salisbury absorber.

This concept can be transferred to a rectangular waveguide transmission line. The difference mainly comes from the impedance Z_s , calculated using (1)-(2), which is no more constant and equal to 377Ω but that is varying as a function of frequency:

$$f_c = \frac{c}{2a} \quad (1)$$

$$Z_S = \frac{\sqrt{\frac{\mu_0}{\varepsilon_0}}}{\sqrt{1 - \left(\frac{f_c}{f}\right)^2}} \quad (2)$$

where c is the light velocity, ε_0 the vacuum permittivity, μ_0 the vacuum permeability, a the waveguide width ($a = 7.11$ mm for a WR-28 waveguide), f_c the TE₁₀ mode cut-off frequency and f the frequency.

As an example, for a WR-28 rectangular waveguide, the impedance of the fundamental mode (TE₁₀) decreases from 573 Ω at 26 GHz to 444 Ω at 40 GHz.

Our objective was to design and manufacture a load based on this resonant absorber by using FDM. However, the resistive layer cannot be 3D-printed. Thus, we replaced it with a layer of lossy ABS-ESD that acts as an absorption and matching layer. Its thickness τ was fixed to 0.1 mm.

The spacer has to be realized with a low-loss dielectric. We selected an ABS material from 3DFilTech. Its dielectric properties were extracted by using a rectangular waveguide method: $\varepsilon_r = 2.6$ and $\tan\delta = 6.10^{-3}$. The guided wavelength λ_g in a rectangular waveguide can be calculated by using:

$$\lambda_g = \frac{c}{f\sqrt{\varepsilon_r}\sqrt{1 - \left(\frac{f_c}{f}\right)^2}} \quad (3)$$

Thus, considering the dielectric properties of ABS in a WR-28 waveguide, the quarter wavelength spacer has to be 1.59-mm long at 36 GHz. However, this length has to be adjusted due to the influence of the dielectric properties of the ABS-ESD layer.

Finally, an ABS-ESD flange was integrated in the design below the bilayer absorber in order to get a component that can be directly connected to a standard metallic waveguide. The topology is presented in Fig. 6. Simulations show that the frequency of maximum absorption logically decreases as the spacer length increases. The resonance frequency is 36.3 GHz for $e_s = 1.6$ mm, a value close to the previously calculated length. Moreover, this spacer length allows achieving specifications.

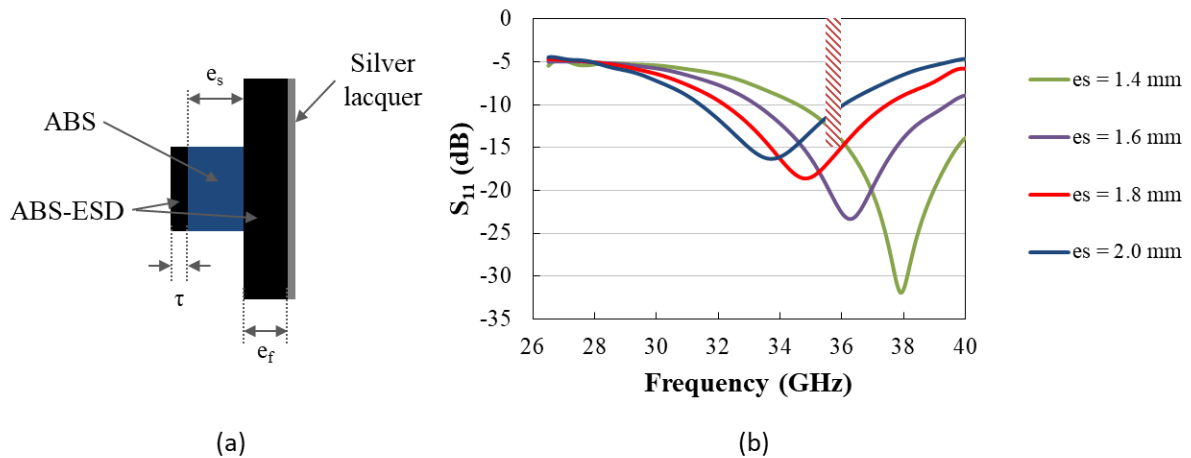


Fig. 6. (a) Side view of the resonant load and (b) amplitude of simulated reflection coefficient S_{11} in Ka-band for different spacer lengths e_s ($\tau = 0.1$ mm, $e_f = 1$ mm).

These loads were manufactured by printing together ABS and ABS-ESD in a single process. Two samples were manufactured for each spacer length. Then, a silver lacquer was applied at the back face of the components before their measurements.

Measurements are shown in Fig. 7. A quite good agreement is observed between simulated and measured reflection coefficients. Even if a small shift in frequency and minimum reflection levels can be observed between two components printed with the same parameters, specifications are achieved for $e_s = 1.6$ mm. In these conditions, the total length of the component is only 2.7 mm which corresponds to a 47% reduction compared to the wedge load. The mass of this component is only 0.38 g.

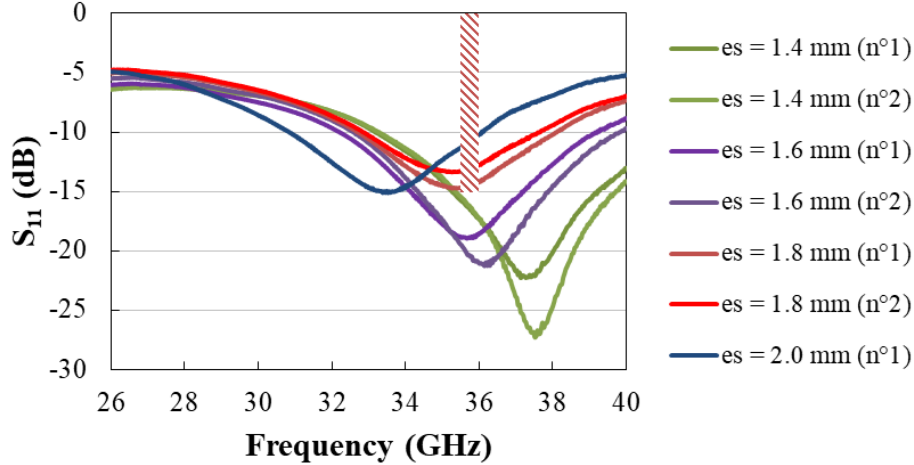


Fig. 7. Measured reflection coefficient S_{11} of resonant loads in Ka-band for different spacer lengths e_s ($\tau = 0.1$ mm, $e_f = 1$ mm). N°1 and n°2 correspond to two different components realized with the same parameters.

CONCLUSION

In this paper, we described the design, manufacturing and measurement of 3D-printed rectangular waveguide loads for Ka-band applications. The objective was to develop a compact low-weight component that can provide a reflection coefficient lower than -15 dB between 35.5 GHz and 36 GHz.

At first, a wedge load based on 3D-printed ABS-ESD was developed. We demonstrated experimentally that a 5.12-mm long component allows achieving these specifications. Moreover, a quite temperature stable behavior was observed between -20°C and 60°C.

Then, a resonant load based on a Salisbury absorber was designed. The components were manufactured by 3D-printing together an absorber material (ABS-ESD) and a low-loss dielectric (ABS). These components proved to respect specifications for a minimum length of 2.7 mm. Thus, a reduction of the length of 47% is achieved with this new topology.

This work thus demonstrated that 3D-printing technologies of microwave absorbers allow developing compact rectangular waveguide loads. The components that were developed are very lightweight (< 0.5g), cheap (filament cost less than 0.1€) and easy to integrate as they are manufactured with their own flanges.

Our current developments are focused on the evaluation of high temperature printable materials such as PEEK, PEKK and PPS that could allow improving thermo-mechanical performance of these components in order to evaluate their integration in satellites.

ACKNOWLEDGEMENTS

This work was supported by the CNES in the framework of the R&T R-S18/TC-0007-120. The authors wish to thank Thales Alenia Space for providing us specifications of the components.

REFERENCES

- [1] Y. Arbaoui, V. Laur, A. Maalouf, P. Queffelec, D. Passerieux, A. Delias, P. Blondy, "Full 3D printed microwave termination: a simple and low cost solution", *IEEE Trans. Micr. Th. & Techn.*, vol. 64, no. 1, pp. 271-278, January 2016.
- [2] A. Maalouf, R. Gingat, V. Laur, "Additive Technology applied to the Realization of K-band Microwave Terminations: Reproducibility Improvement", *Int. J. Micr. Wir. Techn.*, vol. 10, pp. 3-8, February 2018.
- [3] V. Laur, A. Maalouf, A. Chevalier, F. Comblet, "Three-dimensional printing of honeycomb microwave absorbers: Feasibility and innovative multiscale topologies", *IEEE Trans. Electromag. Comp.*, vol. 63, no. 2, pp. 390-397, April 2021.